

# **A novel passive micromixer – lamination in a planar channel system**

**Terje Tofteberg · Maciej Skolimowski · Erik Andreassen · Oliver Geschke**

**Terje Tofteberg · Erik Andreassen**

SINTEF Materials and Chemistry, PO-Box 124 Blindern, 0314 Oslo, Norway

Tel: +47 98624741; Fax: +47 22067350; E-mail: terje.tofteberg@sintef.no

**Maciej Skolimowski · Oliver Geschke**

Technical University of Denmark, Institute for Micro- and Nanotechnology, Building 423 DK-2800 Kgs. Lyngby, Denmark

**Abstract** A novel passive micromixer concept is presented. The working principle is to make a controlled 90 degree rotation of a flow cross section followed by a split into several channels; the flow in each of these channels is rotated a further 90 degrees before a recombination doubles the interfacial area between the two fluids. This process is repeated until achieving the desired degree of mixing. The rotation of the flow field is obtained by patterning the channel bed with grooves. The effect of the mixers has been studied using computational fluid mechanics and prototypes have been micromilled in poly(methyl methacrylate). Confocal microscopy has been used to study the mixing. Several micromixers working by the principle of lamination have been reported in recent years. However, they require three dimensional channel designs which can be complicated to manufacture. The main advantage with the present design is that it is relatively easy to produce using standard microfabrication techniques while at the same time obtaining good lamination between two fluids.

**Keywords** Passive mixer · mixromixer · confocal microscopy · micromilling · simulations

## 1 Introduction

At high Reynolds numbers (typically  $> 2400$ ) two fluids can readily be mixed by turbulence. In microchannels with cross sections less than one millimeter, this becomes difficult to achieve. For water at room temperature, turbulence in such a channel would require a velocity of several meters per second, which, in most cases, is unfeasible. Mixing of two fluids can still be easily done if the Peclet number is small enough. The Peclet number is defined as the ratio between advection time and diffusion time as  $\text{Pe} = uL/D$ , where  $u$  is a characteristic velocity,  $L$  a characteristic length and  $D$  a characteristic diffusion constant. When  $\text{Pe}$  is small, diffusion is fast compared to advection, meaning that mixing can usually be left to diffusion alone e.g. as in a T-type mixer (Wong et al. 2004). This will be the case if the channels are either very small or the diffusion coefficient very large. In the domain where the Reynolds number is small and the Peclet number is large, mixing becomes difficult. In microchannels this typically occurs if the channel dimensions are between 1 and 1000  $\mu\text{m}$ . Such situations arise not only in microfluidics but can also occur in for example polymer processing and food processing. Consider the old art of croissant baking where the interfacial area between layers of buttered dough is increased exponentially each time as the baker repeatedly rolls the dough and folds it.

In a microchannel stretching and folding can be achieved in active mixers by moving solid elements (Rife et al. 2000; Niu and Lee 2003) or by applying time variant electric fields (Glasgow et al. 2004). Even though active mixers can be very efficient, it is generally a disadvantage that they are complex to manufacture. Stretching and folding in passive mixers can be achieved by splitting a stream in one plane and recombining the split streams in a plane orthogonal to the splitting plane as in the so called caterpillar mixer (Cha et al. 2006; Xia et al. 2006). One disadvantage with the caterpillar mixer is that it has to be made by combining at least two structured parts to achieve the three dimensional structure.

In this report we present a mixing principle that is similar to the stretching and folding by splitting and rejoining seen in the caterpillar mixer, but the mixing is done in a channel structured so that the mixer is completed by just bonding a planar lid on top of the structured channel. Thus, the main advantage of the present mixer when compared with active mixers and the caterpillar mixer is the ease of fabrication. The structures can easily be mass produced using polymer replication techniques such as injection moulding or hot embossing.

To the authors knowledge this is the first time a mixer working by the principle of splitting and recombining in such a simple design is presented. In order to achieve the folding, the flows are rotated 90 degrees between each splitting and rejoining. An example of one such module is shown in Figure 1. In this figure the simulated streamlines are colored according to their origin.

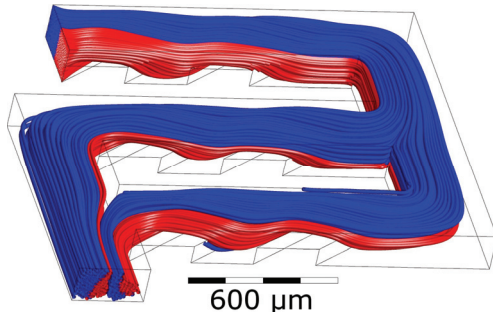


**Fig. 1** Simulated flow field in one mixing module showing lamination.

Other micromixers also function by having ribs rotating the flow field. By patterning at least one of the channel walls it is possible to create rotation of the flow field. It was shown (Stroock et al. 2002), that by creating a staggered herringbone pattern at the channel bed, it is possible to create counter rotating flow fields in a channel. By changing the rotation of the flow when going down the channel very good mixing can be achieved. Several passive 2D mixers have also been proposed working by having obstructions in the flow path creating diverging and merging flow patterns. (Bhagat et al. 2007; Lin et al. 2007; Hsieh and Huang 2008)

The present mixer has been realized using several microfabrication techniques.

- Direct laser ablation of channels and grooves in poly(methyl methacrylate) (PMMA)
- Direct micromilling in polycarbonate (PC) and PMMA
- Milling of the negative structure in aluminium and replication with injection molding in polystyrene (PS)
- Milling of the negative structure in PMMA and replication in polydimethylsiloxane (PDMS)

The results presented in this article relate to mixers milled directly in PMMA. We want to emphasize that the design, because of its open structure and lack of intricate details, can easily be realized using a range of microfabrication techniques.

## 2 Procedure

### 2.1 Microfabrication

As a main fabrication method micromilling (Mini-Mill/3PRO, Minitech Machinery Corp., USA) in PMMA (Röhm GmbH & Co. KG, Germany) was used. First, channels with depth 50  $\mu\text{m}$  and width 300  $\mu\text{m}$  (equal to the diameter of the tool) were milled. In the bed of the channels 200  $\mu\text{m}$  wide grooves were fabricated using a  $\varnothing 100 \mu\text{m}$  milling tool. This tool diameter was chosen to minimize the fillet radius on the corners of the grooves. Cut feed speed was 70 mm/min and spindle rotation was 4000 RPM.

As an alternative fabrication method laser ablation (48-5S Duo Lase carbon dioxide laser, SYNRAD Inc., USA) was used. The channels were obtained using a 10 W laser beam (wavelength 10.6  $\mu\text{m}$ ) and a focusing lens with 200 mm focal length (beam diameter 290  $\mu\text{m}$ ). The ablation velocity was adjusted to 300  $\text{mm}\cdot\text{min}^{-1}$ . For ablation of 200  $\mu\text{m}$  grooves, an 80 mm focal length lens was used (beam diameter 90  $\mu\text{m}$ ) and the power was reduced to 4 W. Ablated structures had a Gaussian-like cross-section as reported earlier (Klank et al. 2002).

The microdevice was sealed with a lid using a silicone adhesive thin film (ARcare® 91005, Adhesive Research Ireland Ltd.). Thermal bonding and laser bonding methods also gave good results.

### 2.2 Confocal laser scanning microscopy measurements

To investigate the performance of the designed micromixer two dyes were used: Rhodamine B and Fluorescein. The dyes were dissolved in phosphate buffered saline (pH = 7.4) with 0.2% sodium dodecyl sulphate (SDS) (all from Sigma-Aldrich Denmark A/S). Confocal laser scanning microscopy (Zeiss LSM 510 Meta, Brock og Michelsen A/S, Denmark) was done using a 40x Fluar oil immersion objective. A 488 nm Argon laser was used for exciting Fluorescein and a 543 nm HeNe laser for Rhodamine B. The pinhole was adjusted for approx. 5  $\mu\text{m}$  z-axis slice thicknesses. The solutions were pumped through the microdevice by a syringe pump (model 540060, TSE Systems GmbH, Germany) with flow rate according to the desired Reynolds number.

### 2.3 Simulations

The mixing efficiency was investigated using 3D finite volume simulations in ANSYS CFX 11.0. The procedure adopted is similar to the one described by Mendels et al (Mendels et al. 2008) where the fluids are treated as isothermal and incompressible Newtonian fluids following the Navier-Stokes equations.

$$\nabla \cdot \mathbf{u} = 0 \quad (1)$$

$$\rho \left[ \frac{\partial \mathbf{u}}{\partial t} + \mathbf{u} \cdot \nabla \mathbf{u} \right] = \nabla p + \eta \nabla^2 \mathbf{u} \quad (2)$$

Here  $\mathbf{u}$  is the velocity vector,  $\rho$  is the density,  $\eta$  the viscosity and  $t$  the time. To track the location of the interface between the two fluids an additional concentration variable  $c$  is transported through the domain by convection and diffusion.

$$\frac{\partial c}{\partial t} + \mathbf{u} \cdot \nabla c = D \nabla^2 c \quad (3)$$

Since the mixer works by lamination, the efficiency of the mixer was best evaluated in the absence of diffusion, therefore the diffusion coefficient,  $D$ , was set to 0 in the simulations.

At the inlet, a sharp step in  $c$  is prescribed, representing two completely separated fluids. Because of numerical diffusion it is necessary to have a fine mesh at the interface between the two phases. This interface is not initially known and in order to define a fine mesh here, an adaptive meshing procedure was used. Equations 1-3 were first solved on a relatively coarse mesh. When convergence was obtained, the mesh was refined where the variation in  $c$  over an element edge exceeded a given value. This procedure was repeated six times with an increasingly finer mesh, until convergence in mesh size. The fluid properties in the simulations are the same as water at 20°C with  $\eta = 1.002 \text{ mPa s}$  and  $\rho = 998 \text{ kg/m}^3$ .

#### 2.4 Validation

To validate the simulations, a channel was made using laser ablation. The geometry was measured using confocal microscopy and the measured geometry was used as a basis for simulations. The resulting rotation can be seen in Fig. 2. It can be seen that there is a good qualitative agreement between the simulated and measured rotation. Using this geometry, the closest thing to a 90° rotation occurs after three grooves. It can also be seen that after six grooves, a full 180° rotation is observed in the simulations. The experimental data indicates that this rotation is taking place already after five grooves. Note also the almost perfect match between the cross section after the first and seventh groove in the simulations. Which is also seen after the first and sixth groove in the experiments.

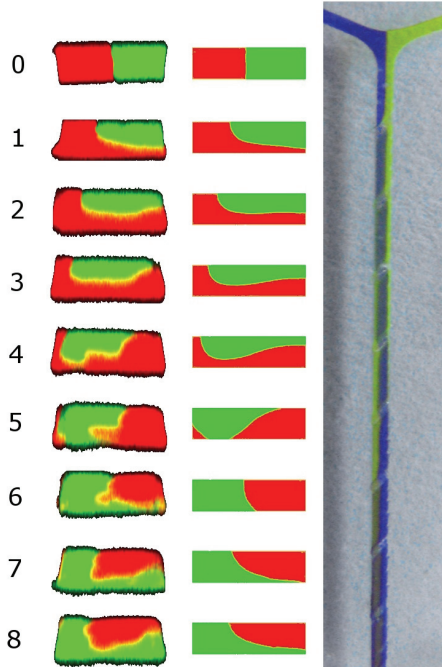


**Fig. 2** Rotation of the flow field in a straight channel with grooves on the channel bed. Left: Confocal fluorescence microscopy measurements of the distribution of rhodamine (red) and Fluorescein (green). Center: Simulated flow field. Right: Photography showing a top view of channel. The numbers indicate the number of grooves.

## 2.5 Design optimization

As can be seen in Figure 2, the rotation after three grooves is not exactly a straight angle. There is also some deformation of the interface between the two tracers, it is no longer a straight line as was the case at the inlet. Three design parameters were varied in a full factorial design to see how a 90° rotation could best be achieved;

- the groove angle( $45^\circ - 55^\circ - 65^\circ$ )
- the depth of the grooves ( $50\mu\text{m} - 100\mu\text{m} - 200\mu\text{m}$ )
- the depth of the channel ( $50\mu\text{m} - 100\mu\text{m} - 200\mu\text{m}$ )

The channel width was fixed to 300  $\mu\text{m}$ . The design optimization was performed using simulations in CFX of straight channels to find the configuration that gave a rotation of the flow as close to 90° as possible. The best results were obtained with a groove angle of 55°, a channel depth of 50  $\mu\text{m}$  and a groove depth of 50  $\mu\text{m}$  which are the parameters used in the following experiments. The design is shown with dimensions in Fig. 3.

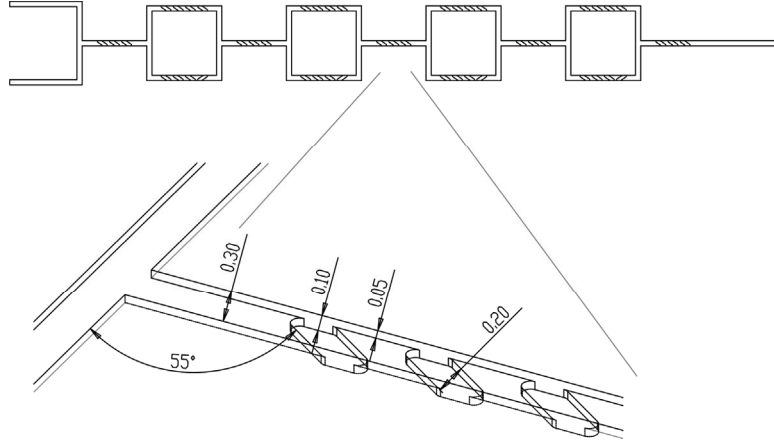
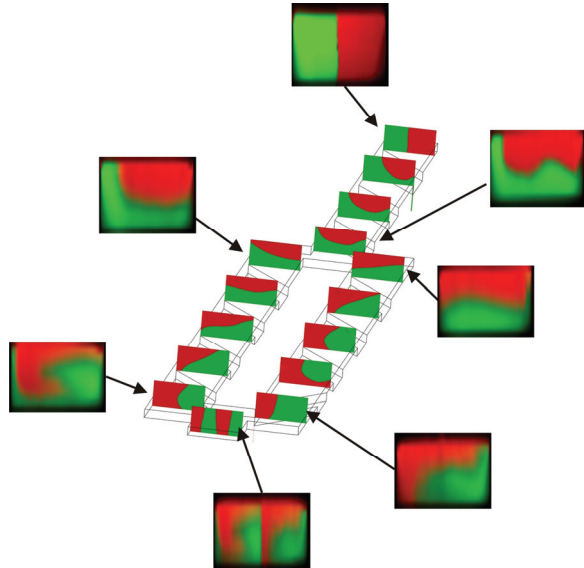


Fig. 3 Above: Design showing four mixing modules. Below: Detailed view of the grooves with dimensions indicated [mm]. The main channel is 50  $\mu\text{m}$  x 300  $\mu\text{m}$  with 50  $\mu\text{m}$  deep, 200  $\mu\text{m}$  wide grooves, inclined 55° relative to the channel axis.

## 3 Results and Discussion

The lamination observed experimentally and in simulations, for one module, is shown in Fig. 4. There is a good agreement between the simulated and measured rotations of the flow field. It is also demonstrated that the mixer is able to laminate the flow field as desired.



**Fig. 4** Concentration distributions within one mixing module. The images on the geometry shows the simulated distribution and the outer ones are confocal microscopy measurements.

The lamination, as measured with confocal microscopy, after one to four modules is shown in Fig. 5a. Note that after three modules the two fluids are mixed well. The different lamina can still be seen, demonstrating that it is the stretching and folding effect of the device that is mixing the fluids. The mixing efficiency will in general be dependent on the Peclet number, showing better mixing at lower Peclet numbers. The diffusion coefficients for Rhodamine B and Fluorescein alone in water is  $3.6 \cdot 10^{-10} \text{ m}^2/\text{s}$  and  $4.9 \cdot 10^{-10} \text{ m}^2/\text{s}$  respectively (Rani et al. 2005). Note that Rhodamine B is hydrophobic and is likely to form micelles with SDS, increasing the diffusion coefficient. This increased diffusion coefficient was not measured. The Peclet number for Fluorescein in the setup shown in **Fig. 5** is 9700.

In the original staggered herringbone article by Stroock et al 2002, the efficiency is evaluated by measuring the standard deviation  $\sigma$  in fluorescence at different locations. The distance required to achieve a reduction in standard deviation by 90 % relative to the inlet,  $\Delta y_{90}$ , is taken as an indication of the length of mixer required. This standard deviation for the present mixer is seen in Fig 3d after one to four full modules and it can be seen that this criteria has been met for the fluorophore with the highest diffusivity, Fluorescein, after four modules. The larger, and slower diffusing rhodamine B is close to achieving this criteria. In Stroock et al this criteria is met after between 3.5 ( $\text{Pe} = 2000$ ) and 8.5 ( $\text{Pe} = 2 \cdot 10^5$ ) rotation cycles. Note that the standard deviation measure for mixing will be dependent on the resolution of the confocal microscopy used and therefor these values for mixing efficiency are not directly comparable from study to study. They are still included here for an indication of the mixing efficiency.

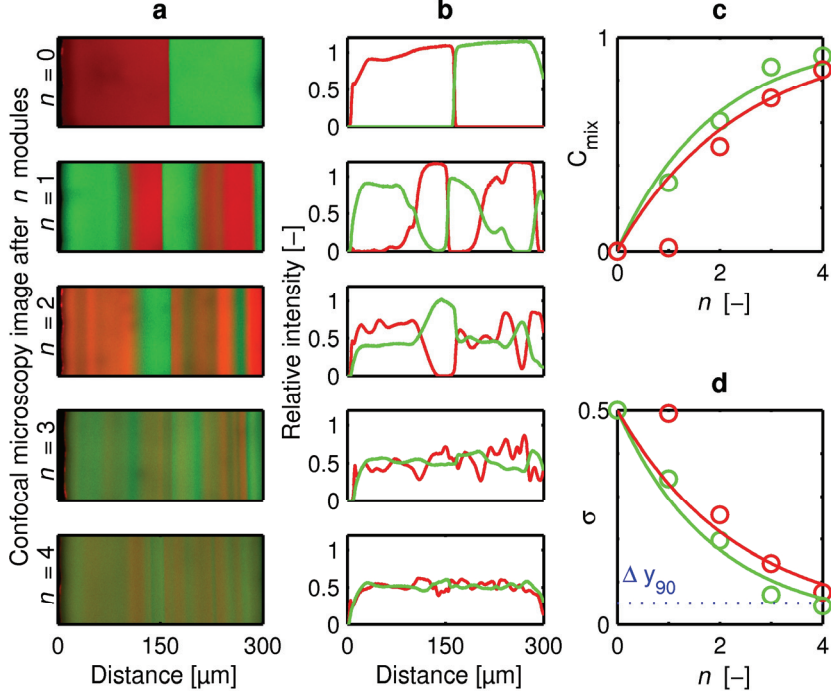


**Fig. 5** **a** Confocal microscopy images showing planes at  $z = h/2$ , where  $h$  is the channel depth. The images show from the top the intensity at the entrance and after one to four full modules. The modules can be seen in Fig. 3. **b** Normalized intensity of the two fluorophores measured across the cross sections in a. **c** The index of mixing evaluated using the variance in the data from b. **d** The standard deviation of the intensities from b including a line showing the criteria used for mixing.

To quantitatively evaluate the mixing efficiency, we define the index of mixing as in (Liu et al. 2004) as

$$C_{\text{mix}} = \frac{\sigma - \sigma_{\text{inlet}}}{\sigma_{\text{inlet}}} \quad (4)$$

where  $\sigma$  is the standard deviation of the fluorescence intensity. They use simulation to evaluate the mixers and sigma is the standard deviation in the concentration of a phase variable. They find that the index of mixing for the herringbone mixer when mixing solutions of glycerol and water is approximately 0.5 ( $\text{Pe} = 1000$ ) after two full mixing cycles. The mixing index for the present mixer is shown in Fig. 5c.

### 3.1 Reynolds number dependence

The simulated lamination for two different Reynolds numbers is shown in Figure 6. Up to a Reynolds number of 5 (flow rate 50 μl/min), changing the flow rate does not change the lamination process. The characteristic length is in this case taken as the hydraulic diameter of the channel (85 μm) and the characteristic velocity is the volume flow divided by the channel cross section (300 μm × 50 μm) where no grooves are present. It can be seen that in the Stokes flow regime, almost perfect lamination is observed. As the momentum effects become more important, however, the rotation of the flow field changes. A further increase in Re, changes the rotation further. The structure still works as a mixer, but the degree of mixing becomes more unpredictable. For the staggered herringbone mixers, which also relies on grooves on the channel bed to rotate the flow field, it has been reported that at high Reynolds numbers (>10) vortices form in the grooves which significantly reduces the rotation (Williams et al. 2008). Similar effects are also seen for three dimensional mixers working by the split and recombine principle, for example, good lamination is only observed with the caterpillar mixers for low Reynolds numbers (<30, (Schonfeld et al. 2004)).

### 3.2 Stacking of design

In this report, the focus has not been on making the design as compact as possible. This can, however, be done when considering the layout in Figure 1. By changing the direction of flow after each rotation of the flow field the overall shape of one mixer module is rectangular. The module shown, measures 1.5 x 1.7 mm and the rectangular overall shape makes it easy to pack it densely on a chip device.

## 4 Conclusions

A new concept for a passive micromixer has been developed. It is shown that the combination of patterning the channel bed and splitting and recombining the streams can be used to make controlled lamination in a 2D channel system. This is shown using both numerical simulations and experiments with prototypes. It is also demonstrated that the design can easily be produced using a range of microfabrication techniques and mass produced using injection molding.

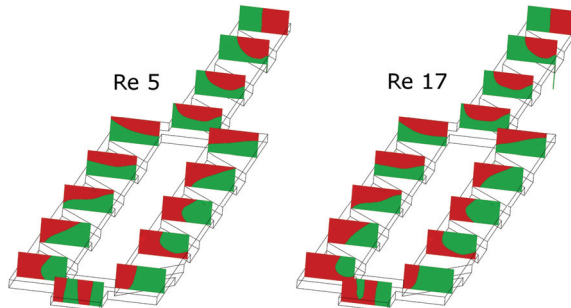


**Fig. 6** Simulated lamination as a function of the Reynolds number. For  $Re < 5$ , the profiles are independent of  $Re$  to the accuracy of this graphical representation.

**Acknowledgements** The idea for the mixer presented in this work originated at the Summer School *Micro mechanical system design and manufacturing* held at the Technical University of Denmark the summer of 2008. We would like to thank the organizers, especially Arnaud De Grave and all students participating for two instructive, hectic and utmost enjoyable weeks in Lyngby. We would also like to thank the Research Council of Norway and the Technical University of Denmark for funding.

## References

- Bhagat AAS, Peterson ETK and Papautsky I (2007) A passive planar micromixer with obstructions for mixing at low Reynolds numbers. *J Micromech Microeng* 17:1017-1024
- Cha J, Kim J, Ryu SK et al (2006) A highly efficient 3D micromixer using soft PDMS bonding. *J Micromech Microeng* 16:1778-1782
- Glasgow I, Batton J and Aubry N (2004) Electroosmotic mixing in microchannels. *Lab Chip* 4:558-562
- Hsieh S-S and Huang Y-C (2008) Passive mixing in micro-channels with geometric variations through  $\mu$ PIV and  $\mu$ LIF measurements. *J Micromech Microeng* 18:065017
- Klank H, Kutter JP and Geschke O (2002) CO<sub>2</sub>-laser micromachining and back-end processing for rapid production of PMMA-based microfluidic systems. *Lab Chip* 2:242-246
- Lin Y-C, Chung Y-C and Wu C-Y (2007) Mixing enhancement of the passive microfluidic mixer with J-shaped baffles in the tee channel. *Biomed Microdevices* 9:215-221
- Liu YZ, Kim BJ and Sung HJ (2004) Two-fluid mixing in a microchannel. *Int J Heat Fluid Flow* 25:986-995
- Mendels DA, Graham EM, Magennis SW et al (2008) Quantitative comparison of thermal and solutal transport in a T-mixer by FLIM and CFD. *Microfluid Nanofluid* 5:603-617
- Niu X and Lee YK (2003) Efficient spatial-temporal chaotic mixing in microchannels. *J Micromech Microeng* 13:454-462
- Rani SA, Pitts B and Stewart PS (2005) Rapid diffusion of fluorescent tracers into *Staphylococcus epidermidis* biofilms visualized by time lapse microscopy. *Antimicrob Agents Chemother* 49:728-732

- Rife JC, Bell MI, Horwitz JS et al (2000) Miniature valveless ultrasonic pumps and mixers. *Sens Actuators, A* 86:135-140
- Schonfeld F, Hessel V and Hofmann C (2004) An optimised split-and-recombine micro-mixer with uniform 'chaotic' mixing. *Lab Chip* 4:65-69
- Stroock AD, Dertinger SKW, Ajdari A et al (2002) Chaotic Mixer for Microchannels. *Science* 295:647-651
- Williams MS, Longmuir KJ and Yager P (2008) A practical guide to the staggered herringbone mixer. *Lab Chip* 8:1121-1129
- Wong SH, Ward MCL and Wharton CW (2004) Micro T-mixer as a rapid mixing micromixer. *Sens Actuators, B* 100:359-379
- Xia HM, Shu C, Wan SYM et al (2006) Influence of the Reynolds number on chaotic mixing in a spatially periodic micromixer and its characterization using dynamical system techniques. *J Micromech Microeng* 16:53-61